Cardiovascular Research (2016) **111**, 84–93
doi:10.1093/cvr/cvw091

Flt-1 (VEGFR-1) coordinates discrete stages of blood vessel formation

John C. Chappell[1,2†], Julia G. Cluceru[1], Jessica E. Nesmith[3], Kevin P. Mouillesseaux[1,4], Vanessa B. Bradley[2], Caitlin M. Hartland[2], Yasmin L. Hashambhoy-Ramsay[5‡], Joseph Walpole[6], Shayn M. Peirce[6], Feilim Mac Gabhann[5], and Victoria L. Bautch[1,3,4,7*]

[1]Department of Biology, The University of North Carolina at Chapel Hill, Chapel Hill, NC 27599, USA; [2]Center for Heart and Regenerative Medicine Research, Virginia Tech Carilion Research Institute, Roanoke, VA 24014, USA; [3]Curriculum in Genetics and Molecular Biology, The University of North Carolina at Chapel Hill, Chapel Hill, NC 27599, USA; [4]Lineberger Comprehensive Cancer Center, The University of North Carolina at Chapel Hill, Chapel Hill, NC 27599, USA; [5]Department of Biomedical Engineering and Institute for Computational Medicine, Johns Hopkins University, Baltimore, MD 21218, USA; [6]Department of Biomedical Engineering, University of Virginia, Charlottesville, VA 22908, USA; and [7]McAllister Heart Institute, The University of North Carolina at Chapel Hill, Chapel Hill, NC 27599, USA

Received 8 March 2015; revised 26 February 2016; accepted 3 March 2016; online publish-ahead-of-print 3 May 2016

Time for primary review: 38 days

Aims In developing blood vessel networks, the overall level of vessel branching often correlates with angiogenic sprout initiations, but in some pathological situations, increased sprout initiations paradoxically lead to reduced vessel branching and impaired vascular function. We examine the hypothesis that defects in the discrete stages of angiogenesis can uniquely contribute to vessel branching outcomes.

Methods and results Time-lapse movies of mammalian blood vessel development were used to define and quantify the dynamics of angiogenic sprouting. We characterized the formation of new functional conduits by classifying discrete sequential stages—sprout initiation, extension, connection, and stability—that are differentially affected by manipulation of vascular endothelial growth factor-A (VEGF-A) signalling via genetic loss of the receptor *flt-1 (vegfr1)*. In mouse embryonic stem cell-derived vessels genetically lacking *flt-1*, overall branching is significantly decreased while sprout initiations are significantly increased. *Flt-1*$^{-/-}$ mutant sprouts are less likely to retract, and they form increased numbers of connections with other vessels. However, loss of *flt-1* also leads to vessel collapse, which reduces the number of new stable conduits. Computational simulations predict that loss of *flt-1* results in ectopic Flk-1 signalling in connecting sprouts post-fusion, causing protrusion of cell processes into avascular gaps and collapse of branches. Thus, defects in stabilization of new vessel connections offset increased sprout initiations and connectivity in *flt-1*$^{-/-}$ vascular networks, with an overall outcome of reduced numbers of new conduits.

Conclusions These results show that VEGF-A signalling has stage-specific effects on vascular morphogenesis, and that understanding these effects on dynamic stages of angiogenesis and how they integrate to expand a vessel network may suggest new therapeutic strategies.

Keywords VEGF-A • Flt-1 • Angiogenesis • ES cells • Computational model

1. Introduction

Vascular endothelial cells undergo elaborate cellular rearrangements to form well-branched blood vessel networks within expanding or remodelling tissues.[1,2] Tissues with insufficient nutrient delivery produce numerous angiogenic factors to induce and coordinate these dynamic cell behaviours.[3] Local and extrinsic patterning cues then guide sprouting endothelial cells as they navigate their environment to ultimately connect and establish new lumenized vessel branches.[4–6] Endothelial cell interactions with one another as well as with soluble and matrix-bound molecular cues such as vascular endothelial growth factor-A (VEGF-A) provide important spatial and temporal regulation to yield

* Corresponding author. Tel: +1 919 966 6797; fax: +1 919 962 4574, E-mail: bautch@med.unc.edu

† Present address. Center for Heart and Regenerative Medicine Research, Virginia Tech Carilion Research Institute, Roanoke, VA 24014, USA.

‡ Present address. Merrimack Pharmaceuticals, Cambridge, MA 02139, USA.

highly ramified vascular networks.[7,8] Increased mechanistic insight into this regulation will likely uncover potential therapeutic targets for treating vascular-related pathologies, including cancer and retinopathy.[9,10]

The receptor tyrosine kinase Flt-1 (VEGF receptor-1) exists as a soluble (sFlt-1) and a membrane-bound (mFlt-1) isoform via messenger RNA alternative splicing.[11] Both isoforms engage VEGF-A with a 10-fold higher binding affinity than Flk-1 (VEGF receptor-2);[12] yet it is Flk-1 activation that induces a range of endothelial cell responses,[13] and Flt-1 signalling in endothelial cells is quite weak and not required for normal vascular development.[14] Thus, developmentally Flt-1 functions primarily as a non-signalling 'reservoir' for VEGF-A by limiting engagement and activation of surface-bound Flk-1 receptors.[15,16] *Flt-1*$^{-/-}$ mutant blood vessels suffer from severe branching dysmorphogenesis,[17] which results in part from loss of Flt-1-dependent endothelial sprout guidance[4,18] and from defects in endothelial cell Notch signalling that require competent Flt-1 activity.[19]

Perturbed VEGF-A signalling leads to changes in blood vessel sprouting, which typically correlates with changes in branching outcomes.[20,21] However, in some vascular beds, genetic loss of *flt-1* or manipulation of Notch signalling significantly reduces vessel branching although sprout initiations are elevated.[19,22–26] Here, we explored this paradox and hypothesized that discrete stages of angiogenic sprouting are differentially affected by loss of *flt-1*, and that these changes integrate to perturb new vessel development. We defined distinct stages of blood vessel formation as a means to analyse time-lapse movies of vascular branching morphogenesis. We found that sprout initiations were increased and had disrupted spatio-temporal organization in *flt-1* mutant vessels and in vessels exposed to excess VEGF-A. *Flt-1*$^{-/-}$ mutant sprouts, once initiated, were less likely to retract and more likely to form new connections, but the stability of new *flt-1*$^{-/-}$ mutant branches over hours was reduced, leading to an overall reduction in branching and fewer new conduits. This work shows via live imaging that the discrete stages within angiogenesis are differentially affected by manipulation of VEGF-A signalling and provides an explanation for the discordance between effects on sprout initiations and final outcomes.

2. Methods

2.1 Cell culture and live imaging

Flt-1$^{-/-}$ (gift of Guo-Hua Fong, University of Connecticut) and wild-type (WT) embryonic stem (ES) cell maintenance and differentiation was described previously.[27] Generation of ES cell lines expressing PECAM-eGFP was previously reported.[28] Dynamic imaging of Day 7–8 differentiating ES cell cultures was performed as follows: confocal images were acquired with either ×10 or ×20 objectives at 4–10 min intervals for 16–20 h using an Olympus FluoView FV1000 or FV10i system, both with environmental chambers. For each scan, a z-stack of 6–8 images was acquired with 4–6 microns between focal planes. Z-stacks were compressed post-acquisition into a single image for each time point. Non-consecutive images are shown for representative movie sequences.

2.2 Quantitative movie analysis

Sprout initiation rate was determined by quantifying the number of sprout initiations, defined as an endothelial cell(s) migrating at least 30 μm away from a parent vessel and remaining extended for at least 30 min (see Supplementary material online, *Figure S1*). Sprout initiation number was divided by movie duration and normalized to overall vessel length for each movie, determined by averaging total vessel lengths for four uniform time points. Outcomes for sprout initiations were scored as *retraction*, defined as a sprout that regressed into the parent vessel, *connection*, defined as a sprout that formed a border with target cells for >1 h, or *undetermined outcome*, when image acquisition ended before a defined outcome. Connections were tracked to determine whether they contributed a stable branch. Unstable connections were further scored for their mode of failure: connection collapse was defined as progressive loss of the avascular gap region formed by connecting endothelial cells; disconnection occurred when an endothelial cell in a stable (>1 h) branch pulled away and regressed into other vessels. For connection collapse, endothelial cells encircling the avascular gap area were scored for active cell protrusions that were clearly distinct from a sprout initiation but still persisted into the avascular area and remained in this space over time, ultimately filling in the avascular region. A blinded observer conducted the connection collapse analysis.

2.3 Sprout initiation cluster analysis and Monte Carlo simulations

A sprout initiation cluster was defined as at least three initiations that were within three to four cell lengths (~300 μm) of each other and occurred within 4 h. The spatial and temporal coordinates (x, y, t) were recorded and a MATLAB algorithm used to determine the total number of sprout clusters per movie. A Monte Carlo simulation of blood vessel sprout initiation was developed to determine whether clustering events were significantly different from expectations based on random sprouting. Briefly, a pixel-value threshold cut-off was applied to a representative vessel image from each movie, and a binary mask used to spatially restrict the area in MATLAB. Time coordinate (t) selection aligned with the time-steps in the movie. The number of sprout initiations was the same for a movie and its corresponding simulation, and the coordinates (x, y, t) were randomly generated, subject to the mask restrictions. The resulting simulation coordinates were evaluated for clustering as for the experimental coordinates. For each movie, the analysis was run five times to obtain mean and standard deviations in a Monte Carlo analysis.

2.4 Partial differential equation simulations

The secretion, diffusion, and binding of VEGF and its receptors were simulated using coupled partial differential equations as described previously,[18] here extended to image-based three-dimensional simulation spaces. Specific images selected from vessel stabilization or collapse sequences were used to define the spatial region for each simulation. Endothelial cells were identified, and in the simulations, each cell expressed mFlt-1, Flk-1, and sFlt-1, and sFlt-1 was secreted from the endothelial cell surface and diffused through non-cellular interstitial space. The endothelial cells were represented as having multiple faces. The representative images are two-dimensional slices through the simulation environment, with the upper surface of the cells shown. It was assumed that a layer of cells below the vessel secreted VEGF-A, and the simulation included reversible binding of VEGF-A and sFlt-1 to the extracellular matrix and to endothelial cell basement membranes. The activation of Flk-1 on the endothelial cell surface resulted from the binding of VEGF to two Flk-1 monomers, while sFlt-1 served as an inhibitor both by sequestering VEGF-A in the interstitial space and by forming heterodimers with VEGF cell surface receptors. To simulate *flt-1*$^{-/-}$ vessels, the expression of both mFlt-1 and sFlt-1 was removed. The resulting distribution of VEGF-A in the interstitial space, and of active Flk-1 on the cell surface, was calculated. Relative and absolute gradients were calculated locally across the interstitial space, or locally on the cell surface for Flk-1.

2.5 Statistical analysis

Statistical analysis was done using SigmaPlot 11 and GraphPad Prism 6. Sprout initiation rates were evaluated by t-test. The Shapiro–Wilk normality test was applied to sprout clustering data, followed by paired t-tests. For sprouting outcomes (retractions, connections, undetermined), unstable sprout connections and their mode of failure, and collapsed connections associated with endothelial cell protrusive activity, we generated five

to six data points for each group (WT, $n = 5$ experiments and *flt-1*$^{-/-}$, $n = 6$ experiments) and compared those values statistically. Each data point was the percentage of a particular sprouting outcome/event for a given movie/experiment. For each outcome/event, we calculated a mean and standard deviation from the five to six data points and compared these data points (i.e. the percentages, $n = 5$ for WT and $n = 6$ for *flt-1*$^{-/-}$) across the two experimental groups by *t*-test. Clustered WT sprout initiation outcomes and connection stability were also evaluated by *t*-test.

3. Results

3.1 Flt-1 limits vessel sprout initiations and regulates their spatio-temporal coordination

Developing ES cell-derived blood vessels lacking *flt-1* have reduced branching, and overgrowth that eventually leads to a 'sheet-like' morphology.[17,28] We hypothesized that genetic deletion of *flt-1* affected sprouting processes in a stage-dependent manner. We analysed mouse ES cells that differentiate into multiple cell types without stimulation towards a specific cell lineage.[27] Endothelial cells form primitive blood vessel networks that expand through angiogenic sprouting and form lumens, processes that mimic blood vessel development *in vivo*.[29] Endothelial cell behaviours were visualized using time-lapse confocal microscopy and ES cell lines that expressed enhanced green fluorescent protein (eGFP) driven by the vascular-specific platelet-endothelial cell adhesion molecule-1 (PECAM-1) promoter.[28] Developing vessel networks derived from WT and *flt-1*$^{-/-}$ ES cells were analysed during periods of robust angiogenesis. To facilitate this analysis, we defined discrete stages of branching morphogenesis that correlated with distinct endothelial cell behaviours—sprout initiation, sprout extension, sprout connection, and sprout stabilization (*Figure 1A*, see Supplementary material online, *Figure S1* and Movie *S1*). These stages were rigorously defined in this study and differ from a previously defined sprout index in several ways, including minimum length, relation to parent vessel, and persistence.[28] We also followed individual sprout initiations and quantified subsequent movement through the stages to outcomes, which was not previously done. Some distinct behaviours, such as lumen formation, were not scored because our labelling strategy did not allow for unambiguous assessment of this parameter.

The rate of sprout initiations was significantly higher in *flt-1*$^{-/-}$ ES cell-derived vessels than WT controls (*Figure 1B–D*, see Supplementary material online, Movies *S2* and *S3*), which is consistent with previous observations of tip cell densities in fixed images.[19] New sprout

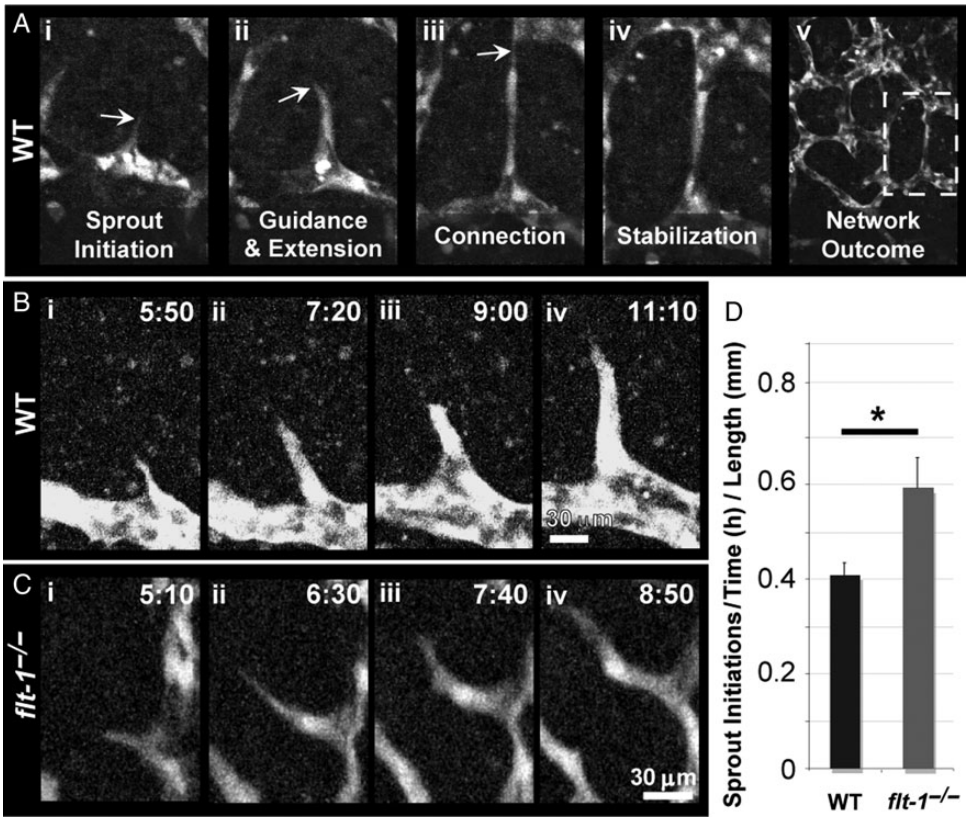

Figure 1 Stages of angiogenesis and effect of loss of *flt-1* on blood vessel sprout initiations. (*A–C*) Representative sequential images from movies of WT and *flt-1*$^{-/-}$ ES cell-derived endothelial cells expressing PECAM-eGFP. (*A*) Overview of the distinct stages of angiogenesis defined by dynamic endothelial cell behaviours—sprout initiation (*Ai*), sprout guidance and extension (*Aii*), sprout connection (*Aiii*), sprout stabilization (*Aiv*)—and the network outcome (*Av*). WT (*B*) and *flt-1*$^{-/-}$ (*C*) endothelial cells migrating further than 30 μm from the initiation site for at least 30 min were counted as sprout initiations, and their location and time of initial sprouting recorded (*Bi–ii* and *Ci–ii*). Sprouts elongating beyond 50 μm and for longer than 60 min were classified as sprout extensions (*Biii–iv* and *Ciii–iv*). Time (h:min), upper right. (*D*) Sprout initiations normalized to time and vessel length for indicated genotypes. Values are averages ± SEM from five to six movies of each genotype. *$P \leq 0.05$ vs. WT using *t*-test comparison.

initiations are spatially and temporally coordinated via integration of several signalling pathways,[19,30–32] so we asked whether loss of *flt-1* disrupted these signalling dynamics. We determined the space-time coordinates (x, y, t) of sprout initiations during live imaging of WT and *flt-1*$^{-/-}$ vessel development (*Figure 2A* and *B*). These coordinates were analysed to identify sprout initiations in close spatio-temporal proximity—specifically, a cluster was defined as a group of three or more initiations, separated by no more than ~300 μm, and by no more than 4 h. We next calculated how many clusters would occur by chance in the absence of an underlying organizing principle using a Monte Carlo simulation (*Figure 2C*). For each movie, we created 1000 sets of randomly generated spatio-temporal coordinates restricted by vessel geometry and movie duration and determined sprout initiation clusters using the criteria for actual initiations. Significantly, more clusters occurred in vessels derived from WT ES cells than expected based on chance, consistent with the concept of an underlying organizing principle, perhaps signalling-related, that regulates vessel sprout initiations in space and time. In contrast, sprout initiation clusters in vessels derived from *flt-1*$^{-/-}$ ES cells were no more prevalent than predicted by chance, suggesting that loss of *flt-1* disrupts the spatio-temporal coordination of blood vessel sprouting.

We next assessed sprout initiations and clustering in a different model of sprouting angiogenesis that allowed for greater temporal control of signalling disruption. We used time-lapse confocal imaging to visualize *flk-1-eGFP*+ endothelial cells within developing blood vessels of explanted mouse embryonic skin (Embryonic Day 14.5). In this *ex vivo* model of sprouting angiogenesis, we modulated VEGF-A signalling activity through application of excess VEGF-A ligand. Although the absolute values for sprout initiation rates and clustering differed slightly from those of ES cell-derived vessels, we found the same trends. Exogenous VEGF-A caused a significant increase in sprout initiations while perturbing their spatial and temporal coordination (see Supplementary material online, *Figure S2* and Movies S4 and S5). Taken together, these data indicate that elevated VEGF-A signalling via excess ligand and genetic loss of *flt-1* both increase the rate of blood vessel sprout initiation and undermine the proper spatio-temporal orchestration of angiogenic sprout initiation, events that are predicted to increase the overall production of productive new branches. Because these two models displayed similar outputs with regard to sprouting dynamics, we focused our remaining analysis on ES cell-derived blood vessels.

3.2 Blood vessel sprout retraction and connection dynamics depend on Flt-1 activity

Because loss of *flt-1* undermines the guidance of blood vessel sprout,[4] we reasoned that misguided *flt-1*$^{-/-}$ sprouts would retract more often and connect less often due to lack of appropriate guidance cues. To investigate these hypotheses, we assessed sprout retractions and connections via live imaging from WT and *flt-1*$^{-/-}$ ES cell-derived vessels (*Figure 3A–D*, see Supplementary material online, Movies S6–S9). WT vessels had 32% of sprouts retract, which is consistent with the presence of collagen IV basement membrane 'sleeves' without vessels in areas of active angiogenesis.[33] To our surprise, only 9% of *flt-1*$^{-/-}$ vessel sprouts retracted, which was significantly less than controls (*Figure 3E–G*). This result suggests that lack of Flt-1-mediated guidance allows some sprouts to avoid a normal retraction process. Moreover, *flt-1*$^{-/-}$ sprouts also connected more frequently with other sprouts and vessels, as 56% of WT sprouts connected during the observation period while 82% of *flt-1*$^{-/-}$ vessel sprouts connected during similar observation periods (*Figure 3E–G*), consistent with *in vivo* observations from zebrafish Flt-1 morphants.[34] The time between sprout initiation and connection or retraction was similar between WT and *flt-1*$^{-/-}$ vessels (see Supplementary material online, *Figure S3*). These findings suggest that, although vessel sprouting could be time-limited in reaching an outcome due to spatial restrictions (e.g. connecting with a nearby vessel), an optimal temporal window for achieving a sprouting endpoint may exist. While this temporal regulation does not appear to require Flt-1 activity, a sprout intrinsic mechanism may control this timing. Thus, loss of *flt-1* prevents sprout retractions and promotes connections, which is predicted to increase vessel branching in the absence of other events.

We extended our analysis of the spatial and temporal clustering found in WT sprout initiations (*Figure 2*) to determine if this phenomenon had any relation to the sprouting outcome. WT sprout initiations

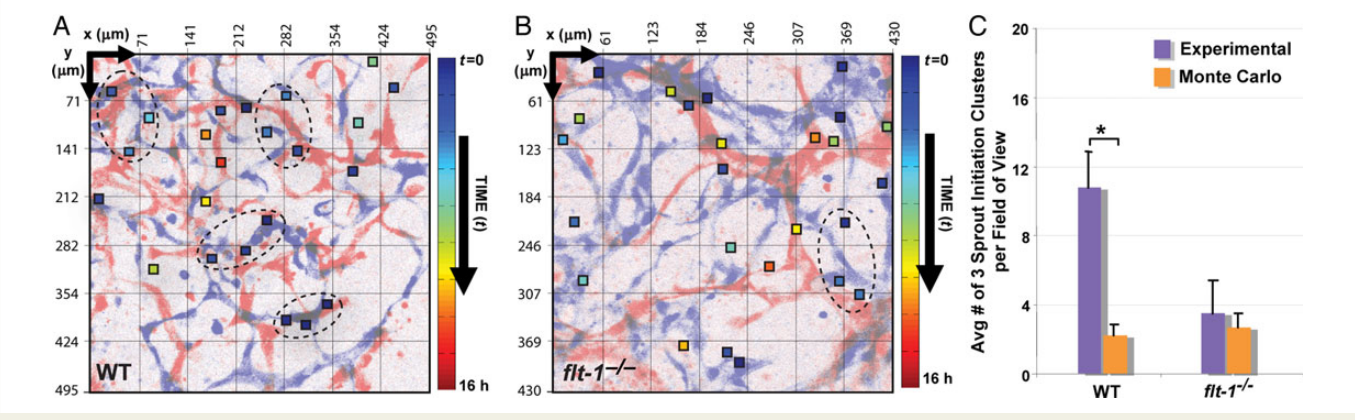

Figure 2 Spatio-temporal organization of sprout initiations is disrupted in *flt-1*$^{-/-}$ vessels. (*A* and *B*) Images taken from a representative region of a WT and *flt-1*$^{-/-}$ movie were recoloured to show time (blue, early; red, late) and superimposed (method: sum). Sprout initiation locations (squares) were colour-encoded for time as shown to the right. Dashed ovals denote a cluster of three sprout initiations. (*C*) Experimentally observed sprout initiation clusters ($n = 5$ movies) compared with clusters in corresponding sets of random coordinates (via Monte Carlo simulation, run 5 times). Values are averages ± SEM from five movies of each genotype. *$P \leq 0.05$ vs. WT experimental using Shapiro–Wilk normality test followed by paired *t*-tests.

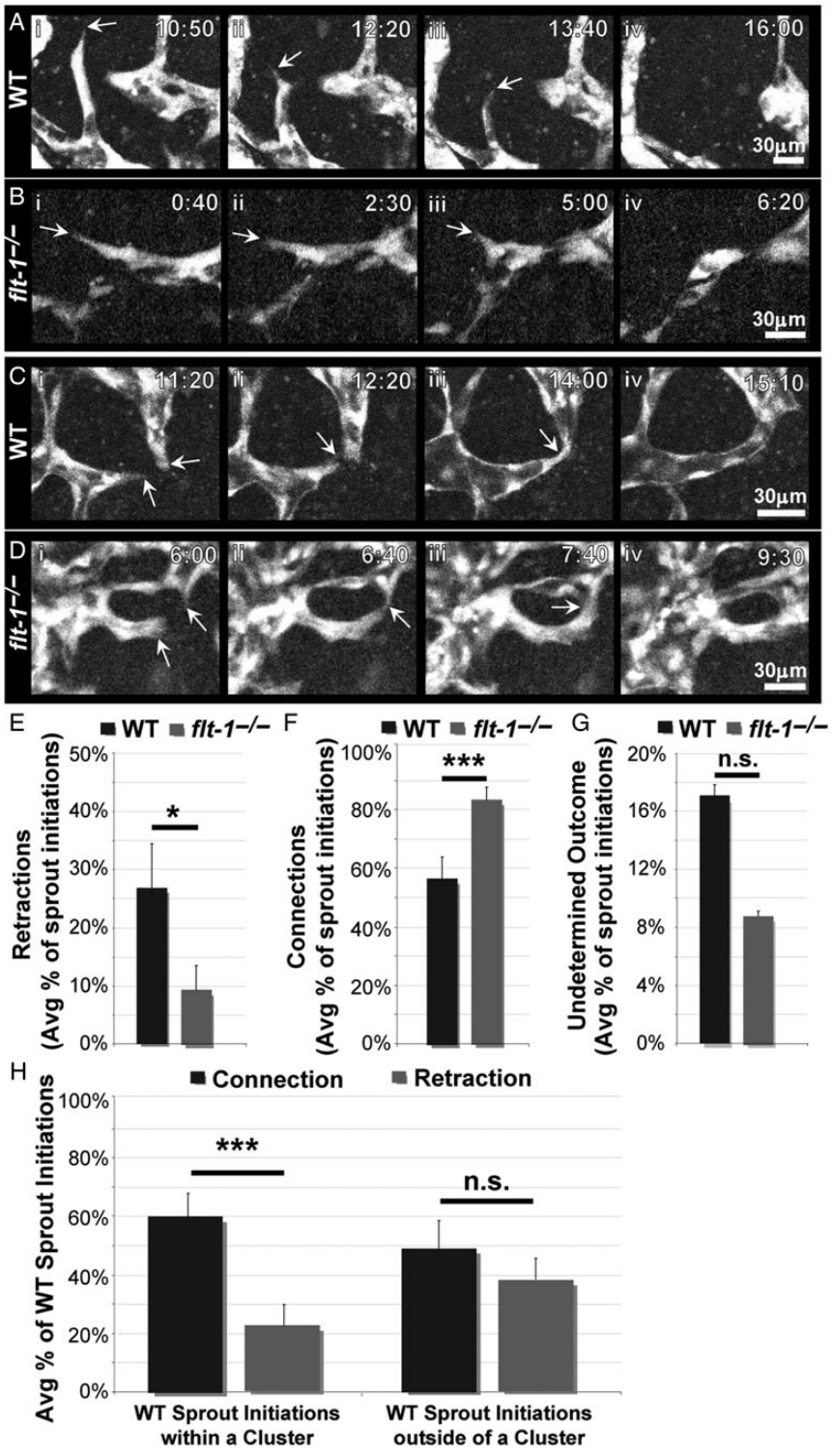

Figure 3 *Flt-1*$^{-/-}$ vessel sprouts have decreased retractions and increased connections, and clustered WT sprout initiations connect more frequently. (*A–D*) Representative time-lapse images of developing vessel networks derived from WT and *flt-1*$^{-/-}$ ES cells expressing PECAM-eGFP in which an endothelial sprout (arrow, *Ai–iii* and *Bi–iii*) retracts into a parent vessel (*Aiv* and *Biv*), and two elongating sprouts (arrows, *Ci* and *Di*) form a connection (arrow, *Cii–iii* and *Dii–iii*). Time (h:min), upper right. (*E–G*) Outcomes for each sprout initiation were assessed (WT: $n = 88$ from five movies, *flt-1*$^{-/-}$: $n = 132$ from six movies), and the percentages of sprouts that retracted (*E*), connected (*F*), or had an undetermined outcome (*G*) were calculated for each movie and averaged. Values are averages $\pm$ SEM from five to six movies of each genotype. In (*E*), *$P \leq 0.05$ vs. WT, in (*F*), ***$P \leq 0.001$ vs. WT, and in (*G*), n.s., not significantly different vs. WT, all using *t*-test comparison. (*H*) Outcomes for each WT sprout initiation were grouped according to its occurrence within or outside a cluster. Percentage of sprouts that connected or retracted were calculated for each group in each movie and averaged. Values are averages $\pm$ SEM from five to six movies of each genotype. ***$P \leq 0.001$ vs. retraction, and n.s., not significantly different vs. retraction, both using *t*-test comparison.

that occurred within a cluster were approximately three times more likely to result in a connection rather than a retraction (*Figure 3H*). However, WT sprout initiations originating outside of a cluster were just as likely to connect as they were to retract, suggesting that there are overlapping 'hot spots' of both sprout initiation and connection.

3.3 Flt-1 promotes the stability of new blood vessel branches

Our system allows tracking of individual newly formed vessels over time to determine their ultimate fate.[27] This analysis showed that some newly formed branches either collapsed into other vessels or broke the connection, so they ultimately did not contribute to overall branching complexity (*Figure 4A* and *B*). In WT networks, ~20% of newly formed branches were unstable, whereas ~45% of new branches formed by *flt-1*$^{-/-}$ vessels were unstable (*Figure 4C*). Intriguingly, all unstable *flt-1*$^{-/-}$ connections failed by vessel collapse, while unstable WT connections failed by both collapse and disconnection, with disconnection being more predominant (*Figure 4D*). These observations demonstrate that loss of *flt-1* destabilizes newly formed vessel connections by enhancing their probability of collapse into nearby vessels, and explains the reduction in new conduits in *flt-1*$^{-/-}$ mutant vessels despite increased sprout initiations and connections.

Given that analysis of WT sprout initiation clustering revealed a correlation between clustered initiations and sprouting outcomes (*Figure 3H*), we asked a similar question about the relationship between sprout clustering and vessel branch stability. Clustered WT sprout initiations were significantly more likely to form stable connections, whereas sprout initiations outside of a cluster were just as likely to be stable as unstable (*Figure 4E*), suggesting that constraints on sprout initiation proximity may also promote stability of nascent vessel connections.

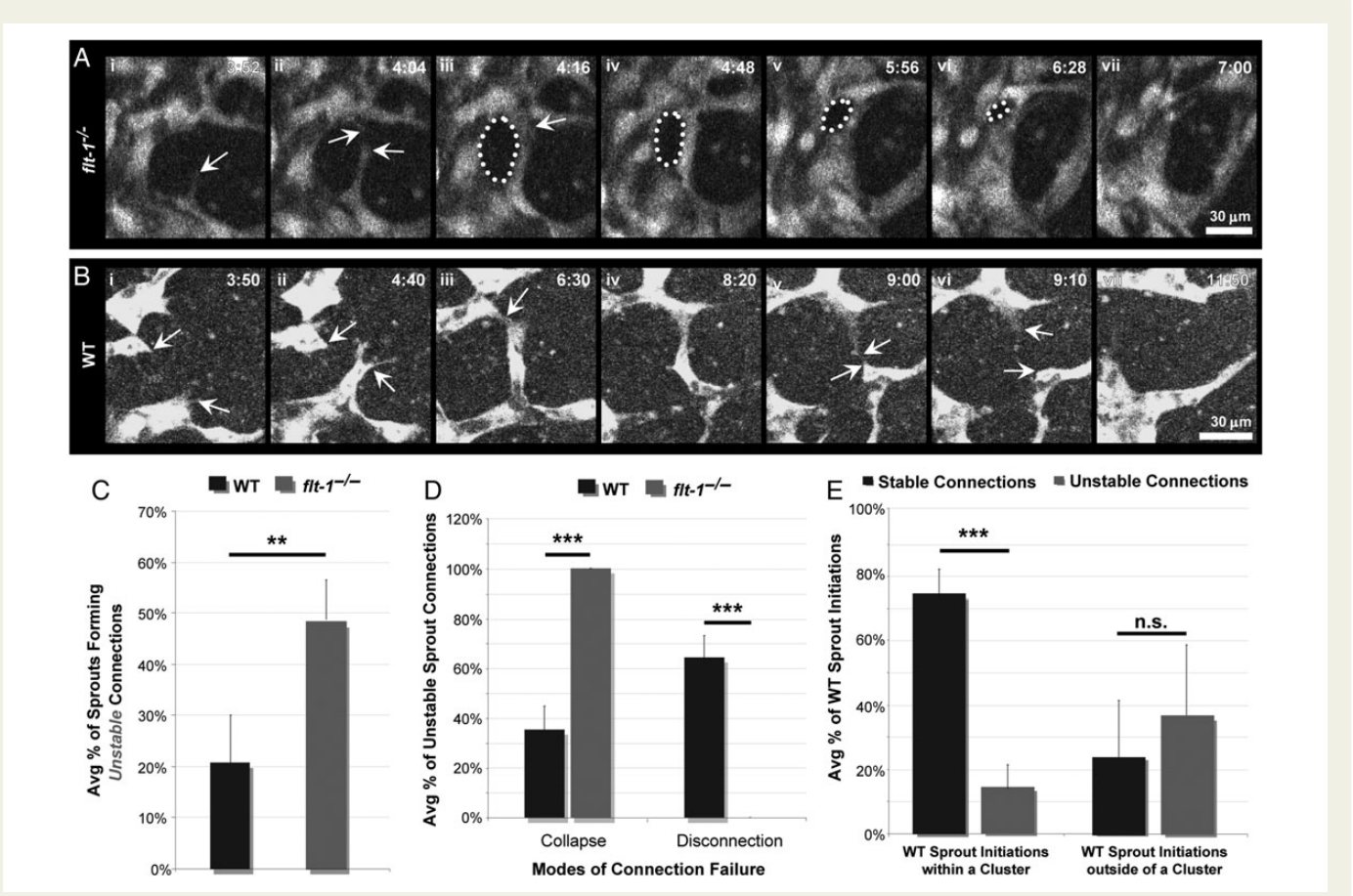

Figure 4 Loss of *flt-1* destabilizes new branches via vessel collapse, and clustered WT sprout initiations have increased branch stability. (*A*) Representative image sequences of PECAM-eGFP vessels derived from *flt-1*$^{-/-}$ ES cells. A new sprout (arrow, *Ai*) engages a target (top arrow, *Aii*) and forms a connection (arrow, *Aiii*). The gap area formed (dotted line, *iii–vi*) collapses over time (*vii*). (*B*) Representative time-lapse images of two WT vessel sprouts (top and bottom arrows, *Bi–ii*) that emerge and form a connection (arrow, *Biii–iv*) until cells within this nascent branch disconnect (*Bv*) and retract (*Bvi–vii*). Time (h:min), upper right. (*C*) New connections formed by WT ($n = 49$ from five movies) or *flt-1*$^{-/-}$ ($n = 107$ from six movies) vessel sprouts were evaluated for stability and ultimate contribution to branching complexity, and percentages were averaged for each movie. Values are averages ± SEM from five to six movies of each genotype. $^{**}P \leq 0.01$ vs. WT using *t*-test comparison. (*D*) The mode of failure (i.e. collapse or disconnection) for each *unstable* connection of indicated genotypes. Percentages were averaged for each movie. Values are averages ± SEM from five to six movies of each genotype. $^{***}P \leq 0.005$ vs. WT using *t*-test comparison. (*E*) Connection outcomes for each WT sprout initiation were grouped according to its occurrence within or outside a cluster. Percentage of sprouts that formed stable or unstable connections were calculated for each group in each movie and then averaged. Values are averages ± SEM from five to six movies of each genotype. $^{***}P \leq 0.001$ vs. unstable connection, and n.s., not significantly different vs. unstable connection, both using *t*-test comparison.

3.4 Flt-1 maintains vessel branches by restricting endothelial cell movement into avascular regions

Loss of *flt-1* spatially alters VEGF-A signalling through the Flk-1 receptor.[15,18] Therefore, we hypothesized that newly formed branches used Flt-1 to spatially modulate VEGF-A activity and promote stabilization of new connections. We coupled live imaging observations with computational modelling of VEGF-A signalling, using still-frames from movies with emerging sprouts that connected with other vessels to form new branches.[18] We reconstructed the cellular architecture of each image in the simulation (*Figure 5Ai–ii* and *Av–vi*), then used this architecture as the boundary condition for partial differential equations that govern diffusion of soluble molecules and the kinetics of VEGF-A ligand–receptor binding events.[18] The simulations showed that after sprout fusion, overall Flk-1 signalling is higher in *flt-1*$^{-/-}$ vessels than WT; in addition, the gradient in Flk-1 signalling is normally low in vessels next to avascular gaps but is elevated in *flt-1*$^{-/-}$ vessels with this topology (*Figure 5Aiii–iv* and *Avii–viii*, arrows). Immunostaining of Flk-1 in presumably recent vessel connections is consistent with these results, showing Flk-1 localization along a single side of a WT connection but encircling the entire avascular gap of a *flt-1*$^{-/-}$ connection (see Supplementary material online, *Figure S4*). The finding that Flk-1 is mis-localized and levels increased suggests that Flt-1 influences both the levels and the spatial distribution of activated Flk-1 bound to VEGF-A. Taken together, the modelling suggests that once endothelial cells connect and form a new branch, Flt-1 dampens Flk-1 signalling at the edge of avascular zones, reducing the likelihood of collapse, and thus promoting new conduits.

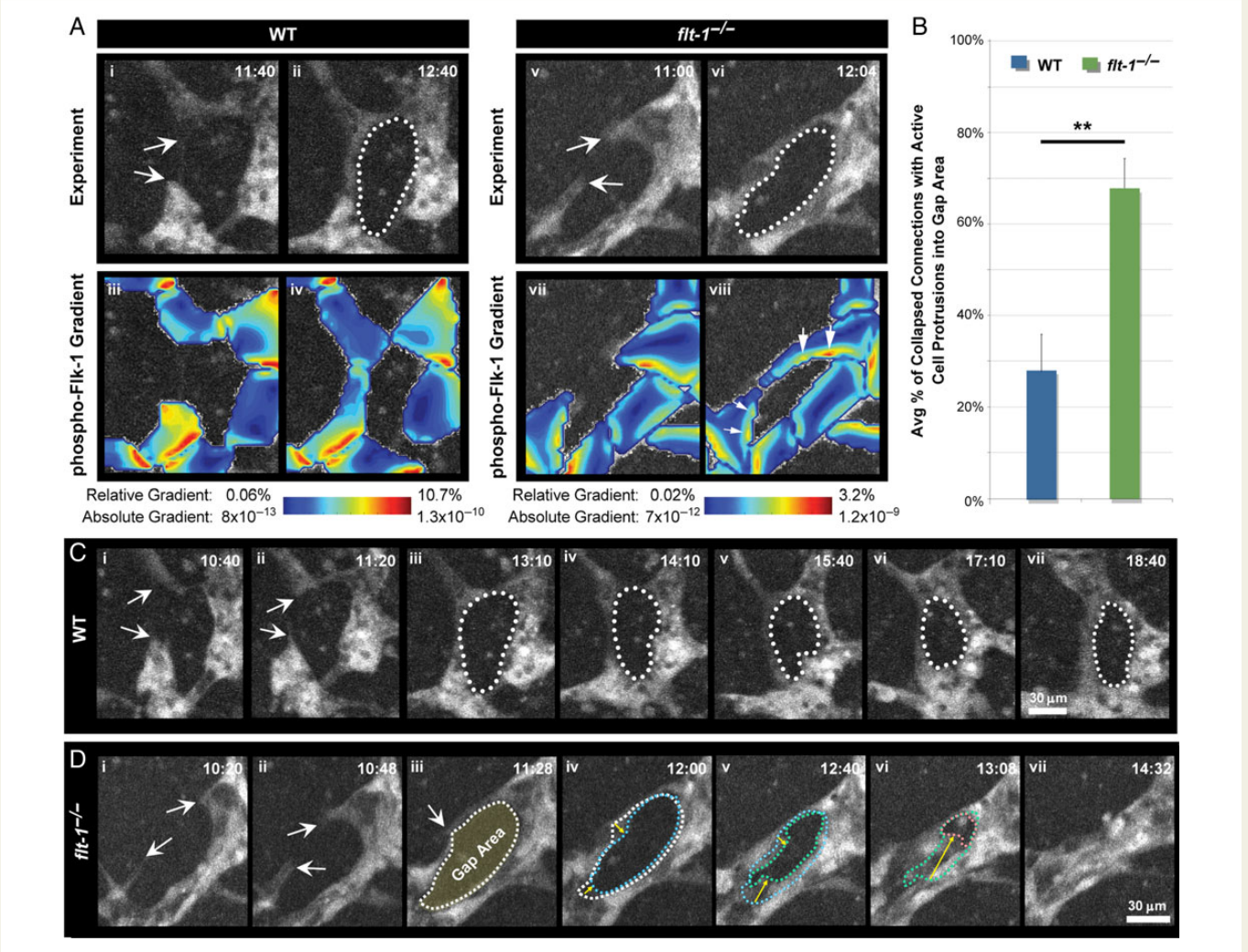

Figure 5 *Flt-1*$^{-/-}$ endothelial cells persistently protrude between branches. (*A*) Representative image sequences of vessel sprouts derived from PECAM-eGFP WT and *flt-1*$^{-/-}$ ES cells as they extend (arrows, *Ai* and *Av*, respectively), connect, and form gap areas (dotted lines, *Aii* and *Avi*). Time (h:min), upper right. The images provided the model geometry for partial differential equation-based simulations of pFlk-1 levels and gradients (*Aiii–iv* and *Avii–viii*), colour-coded as indicated. Arrows, increased pFlk-1 gradients (*Aviii*). (*B*) Areas between branches scored for active endothelial cell protrusions in experimental images from WT ($n = 20$ from five movies) and *flt-1*$^{-/-}$ ($n = 50$ from six movies) vessels. Percentage of collapsed connections with cell protrusions were calculated for each movie and then averaged. Values are averages ± SEM from five to six movies of each genotype. $^{**}P \leq 0.01$ vs. WT using *t*-test comparison. (*C*) Example of stable connection and persistent gap area from vessel sprouts derived from WT ES cells (arrows, *Ci–ii*; dotted line, *Ciii–vii*). (*D*) Example of vessel sprouts derived from *flt-1*$^{-/-}$ ES cells (arrows, *Di–ii*) forming a connection and avascular gap (arrow and dotted line, *Diii*), and undergoing collapse (dotted lines and yellow arrows, *Div–vi*).

These observations led us to hypothesize that loss of *flt-1* increases protrusive endothelial cell activity into avascular areas, due to the elevated Flk-1 signalling predicted by the modelling. We examined WT and *flt-1*$^{-/-}$ ES cell-derived vessel networks where new branches had formed and asked whether subsequent collapse was correlated with persistent protrusive activity into the avascular region. In *flt-1*$^{-/-}$ vessels, 76% of regions in new branches had continuously protrusive endothelial cells (*Figure 5B* and *D*; see Supplementary material online, Movie S10). In contrast, newly formed branches in WT vessels were often maintained (*Figure 5C*), but when they did collapse, significantly fewer (35%) had persistently protrusive and migratory endothelial cells (*Figure 5B*; see Supplementary material online, Movie S11). These data suggest that *flt-1* loss promotes vessel collapse and overall reduction of new conduits by limiting persistent endothelial cell protrusive movement into avascular regions.

4. Discussion

Most defects in blood vessel formation are defined by the final phenotype using static images of fixed tissues. Here, we used live imaging to better understand the dynamic endothelial cell behaviours that contribute to vessel network formation, and we analysed the complex process of sprouting angiogenesis with respect to elemental behaviours or stages (*Figure 1A*). These angiogenic stages are differentially affected by disruption of VEGF-A signalling through excess VEGF-A ligand or genetic deletion of *flt-1*, and an apparent paradox in increased sprout initiations vs. reduced numbers of new conduits in *flt-1*$^{-/-}$ mutant and VEGF-A-saturated blood vessels is explained. This dissection of stage-specific effects also suggests novel points of therapeutic intervention; for example, if the collapse of a new branch were prevented by spatial down-regulation of VEGF-A signalling in vessels surrounding avascular gaps, the overall effect of increased VEGF-A signalling in this and related vascular beds might be to increase new conduits.

Although loss of *flt-1* leads to an increase in tip cell formation[19,35] and sprout initiations (this work), the number of new conduits formed in *flt-1*$^{-/-}$ networks is reduced. Fong *et al.* showed that new conduit formation is significantly impaired in developing mice lacking *flt-1* function,[17] but the cellular basis for this phenotype was unclear. Tumours and wounds subjected to Notch signalling manipulations also have increased tip cells but fewer new conduits.[22–24] In the absence of live imaging, the exact cell behaviours that are affected by these perturbations are unclear. Our live image analysis of *flt-1*$^{-/-}$ mutant vessels suggests that multiple stages of angiogenesis are affected by loss of *flt-1*, but that reduced stabilization of new connections is dominant over effects on other stages such as sprout initiations and connections, leading to overall reduction of new conduits (*Figure 6*).

Our data suggest that blood vessel sprout initiations are regulated in space and time. This regulation may affect whether developing vessels contribute positively to formation of new conduits, since ectopic VEGF-A or loss of *flt-1* randomized the location of initiations, perhaps leading to connections in inappropriate locations that contributed to the high rate of collapse of *flt-1*$^{-/-}$ mutant branches. Further, supporting this idea is our finding that clustered WT sprout initiations more often resulted in stable connections than did sprout initiations outside of

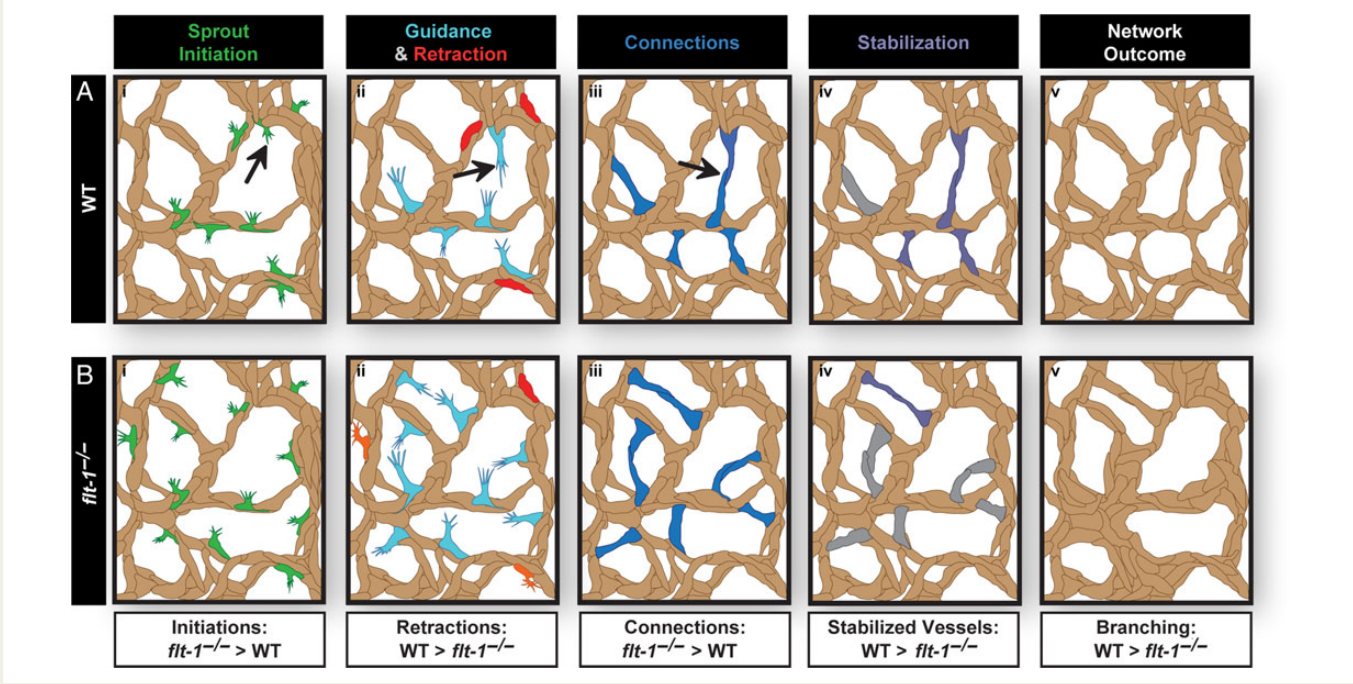

Figure 6 Stages of branching compromised by loss of *flt-1* during angiogenesis. (*A*) During normal blood vessel development, endothelial cells (tan) initiate new vessel sprouts (green, *Ai*). A subset of these sprouts retract back into their original location (red, *Aii*), while those that continue extending form connections with target areas (blue, *Aiii*). Occasionally, a new connection fails to contribute to the overall branching complexity of the network, such as through vessel collapse (grey, *Aiv*), but generally these stages yield stable branches (purple, *Aiv*) and an increase in vascular branching (*Av*). (*B*) Loss of *flt-1* leads to aberrant increases in sprout initiation (green, *Bi*). *Flt-1*$^{-/-}$ vessel sprouts retract less often than WT sprouts (red, *Bii*), but a portion fail to extend due to defects in sprout guidance (orange, *Bii*).[4] Vessel sprouts form connections with other sprouts or vessels excessively (blue, *Biii*), yet these connections often fail by collapsing into adjacent structures (grey, *Biv*). Defects arising during each stage of *flt-1*$^{-/-}$ vessel development accumulate and undermine network complexity (*Bv*).

clusters. Local cues that promote sprout clustering may also enhance sprout connection and branch stability, and perhaps sprouts connecting directly with one another yield more stable branches when compared with those fusing with an existing vessel segment. These observations are in agreement with previous studies showing that VEGF signalling is involved in spatial regulation of vascular branching morphogenesis, likely via integration with Notch signalling.[19,30] During *Drosophila* trachea development, branch formation is similarly spatially coordinated by fibroblast growth factor signalling that is modulated by Notch,[32] demonstrating that mechanisms for patterning new conduits are conserved across tissues and organisms.[31] Recent work suggests that, within a local area, the precise location of a vascular sprout initiation also depends on flow parameters,[36] suggesting that mechanical cues integrate with molecular signalling cues in flow-dependent models. Our results highlight that tight spatio-temporal regulation of vessel sprout initiations is likely important in the formation of appropriately branched vascular networks.

Angiogenesis studies that include time-lapse analysis of blood vessel formation often focus on sprouting in stereotyped vascular beds such as zebrafish intersegmental vessels, where retraction has not been well described.[37,38] We show that in WT mammalian vessels, sprout initiations sometimes fully retract into the parent vessel. These dynamic behaviours are consistent with reports of collagen IV 'sleeves' of basement membrane that remain in the absence of vessels, presumably following capillary sprout retraction or remodelling.[39,40] This retraction mode of network formation is also important for axonal branching and patterning, particularly during wound healing following spinal cord injury.[41] Loss of *flt-1* decreases the likelihood of angiogenic sprout retraction and increases the connection rate. This is likely due to tip cells experiencing excess VEGF-A signalling, which may in turn inappropriately reinforce sprout extensions and connections. Thus, when VEGF-A signalling is mis-regulated, such as in solid tumours, vascular dysmorphogenesis is likely exacerbated by decreased sprout retraction and increased sprout connections.

A surprising finding was that the stability of newly formed branches is a critical stage of blood vessel development compromised by genetic loss of *flt-1*. Computational simulations of new branches with and without Flt-1 activity predicted higher levels of Flk-1 activation in areas near gaps between mutant sprouts, and this correlated with increased endothelial cell protrusive activity, a behaviour consistent with hyperactive Flk-1 signalling.[42] Previous *in vivo* studies in quail embryos showed that high VEGF-A reduces branching complexity by promoting vessel coalescence,[43] which we also observe in the developing zebrafish liver plexus exposed to excess Vegfaa (see Supplementary material online, *Figure S5*). More recently, it was shown that *in vivo* blood flow through mouse yolk sac vessels also modulates branch maintenance and vessel fusion,[44] which represents another mechanism for further refinement of a developing vessel plexus. In non-stereotypical vascular networks, the location of sprout connections may also be important in determining which connections are maintained and which are lost. Flt-1-mediated modulation of VEGF signalling is thus essential to regulate sprout initiation and guidance,[4] and also stability of new branches, likely by regulating spatial aspects of Flk-1 signalling after a connection is formed.

Defining distinct stages of sprouting angiogenesis via live imaging shows how loss of *flt-1* elevates sprout initiations and connections yet ultimately leads to reduced branching complexity in our model, which mimics developmental angiogenesis in unrestrained vascular beds such as the yolk sac.[19,22–24,26] The finding of differential effects of *flt-1* loss on distinct stages of angiogenesis also provides an explanation for different phenotypes associated with *flt-1* loss in different vascular beds. For example, Ho *et al.* recently showed that conditional loss of *flt-1* led to increased vascular branching in the developing mouse retina;[45] this observation contrasts with *flt-1* global knockout and VEGF-A gain-of-function phenotypes described in other tissues such as the embryonic yolk sac and mouse skeletal muscle.[17,43,46] We propose that the collapse of new branches so prevalent in our system is prevented in the retina by the astrocyte network that stabilizes new branches independent of Flt-1, making dominant the effects of *flt-1* loss on earlier angiogenic stages. In this way, a better understanding of how particular pathways affect distinct dynamic stages of blood vessel formation will improve predictions of therapeutic efficacy when treating a given vascular bed.

Supplementary material

Supplementary material is available at *Cardiovascular Research* online.

Acknowledgements

The authors thank the Bautch Lab members for stimulating discussion during manuscript preparation.

Conflict of interest: none declared.

Funding

This work was supported by the National Institutes of Health (R01HL43174 to V.L.B.; F32HL95359 and K99HL105779 to J.C.C.; and R00HL093219 to F.M.G.), the American Heart Association (12BGIA12060154 to F.M.G.), and a Sloan Research Fellowship (to F.M.G.).

References

1. Bentley K, Franco CA, Philippides A, Blanco R, Dierkes M, Gebala V, Stanchi F, Jones M, Aspalter IM, Cagna G, Westrom S, Claesson-Welsh L, Vestweber D, Gerhardt H. The role of differential VE-cadherin dynamics in cell rearrangement during angiogenesis. *Nat Cell Biol* 2014;**16**:309–321.
2. Siekmann AF, Affolter M, Belting HG. The tip cell concept 10 years after: new players tune in for a common theme. *Exp Cell Res* 2013;**319**:1255–1263.
3. Logsdon EA, Finley SD, Popel AS, Mac Gabhann F. A systems biology view of blood vessel growth and remodelling. *J Cell Mol Med* 2014;**18**:1491–1508.
4. Chappell JC, Taylor SM, Ferrara N, Bautch VL. Local guidance of emerging vessel sprouts requires soluble Flt-1. *Dev Cell* 2009;**17**:377–386.
5. Lenard A, Ellertsdottir E, Herwig L, Krudewig A, Sauteur L, Belting HG, Affolter M. In vivo analysis reveals a highly stereotypic morphogenetic pathway of vascular anastomosis. *Dev Cell* 2013;**25**:492–506.
6. Xu K, Cleaver O. Tubulogenesis during blood vessel formation. *Semin Cell Dev Biol* 2011;**22**:993–1004.
7. Dorrell MI, Friedlander M. Mechanisms of endothelial cell guidance and vascular patterning in the developing mouse retina. *Prog Retin Eye Res* 2006;**25**:277–295.
8. Vieira JM, Ruhrberg C, Schwarz Q. VEGF receptor signaling in vertebrate development. *Organogenesis* 2010;**6**:97–106.
9. Potente M, Gerhardt H, Carmeliet P. Basic and therapeutic aspects of angiogenesis. *Cell* 2011;**146**:873–887.
10. Luttun A, Tjwa M, Moons L, Wu Y, Angelillo-Scherrer A, Liao F, Nagy JA, Hooper A, Priller J, De Klerck B, Compernolle V, Daci E, Bohlen P, Dewerchin M, Herbert JM, Fava R, Matthys P, Carmeliet G, Collen D, Dvorak HF, Hicklin DJ, Carmeliet P. Revascularization of ischemic tissues by PlGF treatment, and inhibition of tumor angiogenesis, arthritis and atherosclerosis by anti-Flt1. *Nat Med* 2002;**8**:831–840.
11. He Y, Smith SK, Day KA, Clark DE, Licence DR, Charnock-Jones DS. Alternative splicing of vascular endothelial growth factor (VEGF)-R1 (FLT-1) pre-mRNA is important for the regulation of VEGF activity. *Mol Endocrinol* 1999;**13**:537–545.
12. Waltenberger J, Claesson-Welsh L, Siegbahn A, Shibuya M, Heldin CH. Different signal transduction properties of KDR and Flt1, two receptors for vascular endothelial growth factor. *J Biol Chem* 1994;**269**:26988–26995.
13. Koch S, Claesson-Welsh L. Signal transduction by vascular endothelial growth factor receptors. *Cold Spring Harb Perspect Med* 2012;**2**:a006502.

14. Hiratsuka S, Minowa O, Kuno J, Noda T, Shibuya M. Flt-1 lacking the tyrosine kinase domain is sufficient for normal development and angiogenesis in mice. *Proc Natl Acad Sci USA* 1998;**95**:9349–9354.
15. Kappas NC, Zeng G, Chappell JC, Kearney JB, Hazarika S, Kallianos KG, Patterson C, Annex BH, Bautch VL. The VEGF receptor Flt-1 spatially modulates Flk-1 signaling and blood vessel branching. *J Cell Biol* 2008;**181**:847–858.
16. Roberts DM, Kearney JB, Johnson JH, Rosenberg MP, Kumar R, Bautch VL. The vascular endothelial growth factor (VEGF) receptor Flt-1 (VEGFR-1) modulates Flk-1 (VEGFR-2) signaling during blood vessel formation. *Am J Pathol* 2004;**164**:1531–1535.
17. Fong GH, Rossant J, Gertsenstein M, Breitman ML. Role of the Flt-1 receptor tyrosine kinase in regulating the assembly of vascular endothelium. *Nature* 1995;**376**:66–70.
18. Hashambhoy YL, Chappell JC, Peirce SM, Bautch VL, Mac Gabhann F. Computational modeling of interacting VEGF and soluble VEGF receptor concentration gradients. *Front Physiol* 2011;**2**:62.
19. Chappell JC, Mouillesseaux KP, Bautch VL. Flt-1 (vascular endothelial growth factor receptor-1) is essential for the vascular endothelial growth factor-Notch feedback loop during angiogenesis. *Arterioscler Thromb Vasc Biol* 2013;**33**:1952–1959.
20. Wang Y, Nakayama M, Pitulescu ME, Schmidt TS, Bochenek ML, Sakakibara A, Adams S, Davy A, Deutsch U, Luthi U, Barberis A, Benjamin LE, Makinen T, Nobes CD, Adams RH. Ephrin-B2 controls VEGF-induced angiogenesis and lymphangiogenesis. *Nature* 2010;**465**:483–486.
21. Jung B, Obinata H, Galvani S, Mendelson K, Ding BS, Skoura A, Kinzel B, Brinkmann V, Rafii S, Evans T, Hla T. Flow-regulated endothelial S1P receptor-1 signaling sustains vascular development. *Dev Cell* 2012;**23**:600–610.
22. Ridgway J, Zhang G, Wu Y, Stawicki S, Liang WC, Chanthery Y, Kowalski J, Watts RJ, Callahan C, Kasman I, Singh M, Chien M, Tan C, Hongo JA, de Sauvage F, Plowman G, Yan M. Inhibition of Dll4 signalling inhibits tumour growth by deregulating angiogenesis. *Nature* 2006;**444**:1083–1087.
23. Noguera-Troise I, Daly C, Papadopoulos NJ, Coetzee S, Boland P, Gale NW, Lin HC, Yancopoulos GD, Thurston G. Blockade of Dll4 inhibits tumour growth by promoting non-productive angiogenesis. *Nature* 2006;**444**:1032–1037.
24. Al Haj Zen A, Oikawa A, Bazan-Peregrino M, Meloni M, Emanueli C, Madeddu P. Inhibition of delta-like-4-mediated signaling impairs reparative angiogenesis after ischemia. *Circ Res* 2010;**107**:283–293.
25. Li JL, Sainson RC, Shi W, Leek R, Harrington LS, Preusser M, Biswas S, Turley H, Heikamp E, Hainfellner JA, Harris AL. Delta-like 4 Notch ligand regulates tumor angiogenesis, improves tumor vascular function, and promotes tumor growth in vivo. *Cancer Res* 2007;**67**:11244–11253.
26. Pasula S, Cai X, Dong Y, Messa M, McManus J, Chang B, Liu X, Zhu H, Mansat RS, Yoon SJ, Hahn S, Keeling J, Saunders D, Ko G, Knight J, Newton G, Luscinskas F, Sun X, Towner R, Lupu F, Xia L, Cremona O, De Camilli P, Min W, Chen H. Endothelial epsin deficiency decreases tumor growth by enhancing VEGF signaling. *J Clin Invest* 2012;**122**:4424–4438.
27. Kearney JB, Bautch VL. In vitro differentiation of mouse ES cells: hematopoietic and vascular development. *Methods Enzymol* 2003;**365**:83–98.
28. Kearney JB, Kappas NC, Ellerstrom C, DiPaola FW, Bautch VL. The VEGF receptor flt-1 (VEGFR-1) is a positive modulator of vascular sprout formation and branching morphogenesis. *Blood* 2004;**103**:4527–4535.
29. Larina IV, Shen W, Kelly OG, Hadjantonakis AK, Baron MH, Dickinson ME. A membrane associated mCherry fluorescent reporter line for studying vascular remodeling and cardiac function during murine embryonic development. *Anat Rec (Hoboken)* 2009;**292**:333–341.
30. Jakobsson L, Bentley K, Gerhardt H. VEGFRs and Notch: a dynamic collaboration in vascular patterning. *Biochem Soc Trans* 2009;**37**:1233–1236.
31. Affolter M, Zeller R, Caussinus E. Tissue remodelling through branching morphogenesis. *Nat Rev Mol Cell Biol* 2009;**10**:831–842.
32. Ghabrial AS, Krasnow MA. Social interactions among epithelial cells during tracheal branching morphogenesis. *Nature* 2006;**441**:746–749.
33. Mancuso MR, Davis R, Norberg SM, O'Brien S, Sennino B, Nakahara T, Yao VJ, Inai T, Brooks P, Freimark B, Shalinsky DR, Hu-Lowe DD, McDonald DM. Rapid vascular regrowth in tumors after reversal of VEGF inhibition. *J Clin Invest* 2006;**116**:2610–2621.
34. Krueger J, Liu D, Scholz K, Zimmer A, Shi Y, Klein C, Siekmann A, Schulte-Merker S, Cudmore M, Ahmed A, le Noble F. Flt1 acts as a negative regulator of tip cell formation and branching morphogenesis in the zebrafish embryo. *Development* 2011;**138**:2111–2120.
35. Jakobsson L, Franco CA, Bentley K, Collins RT, Ponsioen B, Aspalter IM, Rosewell I, Busse M, Thurston G, Medvinsky A, Schulte-Merker S, Gerhardt H. Endothelial cells dynamically compete for the tip cell position during angiogenic sprouting. *Nat Cell Biol* 2010;**12**:943–953.
36. Ghaffari S, Leask RL, Jones EA. Flow dynamics control the location of sprouting and direct elongation during developmental angiogenesis. *Development* 2015;**142**:4151–4157.
37. Blum Y, Belting HG, Ellertsdottir E, Herwig L, Luders F, Affolter M. Complex cell rearrangements during intersegmental vessel sprouting and vessel fusion in the zebrafish embryo. *Dev Biol* 2008;**316**:312–322.
38. Kamei M, Isogai S, Pan W, Weinstein BM. Imaging blood vessels in the zebrafish. *Methods Cell Biol* 2010;**100**:27–54.
39. Phng LK, Potente M, Leslie JD, Babbage J, Nyqvist D, Lobov I, Ondr JK, Rao S, Lang RA, Thurston G, Gerhardt H. Nrarp coordinates endothelial Notch and Wnt signaling to control vessel density in angiogenesis. *Dev Cell* 2009;**16**:70–82.
40. Ehling M, Adams S, Benedito R, Adams RH. Notch controls retinal blood vessel maturation and quiescence. *Development* 2013;**140**:3051–3061.
41. Dray C, Rougon G, Debarbieux F. Quantitative analysis by in vivo imaging of the dynamics of vascular and axonal networks in injured mouse spinal cord. *Proc Natl Acad Sci USA* 2009;**106**:9459–9464.
42. Gerhardt H, Golding M, Fruttiger M, Ruhrberg C, Lundkvist A, Abramsson A, Jeltsch M, Mitchell C, Alitalo K, Shima D, Betsholtz C. VEGF guides angiogenic sprouting utilizing endothelial tip cell filopodia. *J Cell Biol* 2003;**161**:1163–1177.
43. Drake CJ, Little CD. Exogenous vascular endothelial growth factor induces malformed and hyperfused vessels during embryonic neovascularization. *Proc Natl Acad Sci USA* 1995;**92**:7657–7661.
44. Udan RS, Vadakkan TJ, Dickinson ME. Dynamic responses of endothelial cells to changes in blood flow during vascular remodeling of the mouse yolk sac. *Development* 2013;**140**:4041–4050.
45. Ho VC, Duan LJ, Cronin C, Liang BT, Fong GH. Elevated vascular endothelial growth factor receptor-2 abundance contributes to increased angiogenesis in vascular endothelial growth factor receptor-1-deficient mice. *Circulation* 2012;**126**:741–752.
46. Ozawa CR, Banfi A, Glazer NL, Thurston G, Springer ML, Kraft PE, McDonald DM, Blau HM. Microenvironmental VEGF concentration, not total dose, determines a threshold between normal and aberrant angiogenesis. *J Clin Invest* 2004;**113**:516–527.